Microcanonical temperature for a classical field: Application to Bose-Einstein condensation

M. J. Davis*

ARC Centre of Excellence for Quantum Atom Optics, Department of Physics, University of Queensland, St Lucia, QLD 4072, Australia

S. A. Morgan[†]

Department of Physics and Astronomy, University College London, Gower Street, London WC1E 6BT, United Kingdom

We show that the projected Gross-Pitaevskii equation (PGPE) can be mapped exactly onto Hamilton's equations of motion for classical position and momentum variables. Making use of this mapping, we adapt techniques developed in statistical mechanics to calculate the temperature and chemical potential of a classical Bose field in the microcanonical ensemble. We apply the method to simulations of the PGPE, which can be used to represent the highly occupied modes of Bose condensed gases at finite temperature. The method is rigorous, valid beyond the realms of perturbation theory, and agrees with an earlier method of temperature measurement for the same system. Using this method we show that the critical temperature for condensation in a homogeneous Bose gas on a lattice with a uv cutoff increases with the interaction strength. We discuss how to determine the temperature shift for the Bose gas in the continuum limit using this type of calculation, and obtain a result in agreement with more sophisticated Monte Carlo simulations. We also consider the behavior of the specific heat.

I. INTRODUCTION

The Gross-Pitaevskii equation (GPE) has proven to be an extremely useful description of macroscopic Bose-Einstein condensates (BECs) at or near zero temperature [1]. It is the first and sometimes only tool to be used in the description of many experiments in the field of nonlinear atom optics and Bose-Einstein condensation. The validity of the GPE for many wide-ranging experimental situations now appears beyond doubt.

However, it has been proposed that the GPE can also be used to represent the nonequilibrium dynamics of Bose gases at finite temperature [2–5]. The underlying argument is that, for modes of the gas with an average occupation much larger than 1, the classical dynamics is far more important than the quantum dynamics. This is analogous to the semiclassical approximation utilized in laser physics for the electromagnetic field. A major advantage of using the GPE in such situations is that it is nonperturbative and so can be applied in the region of the critical point as long as the condition on occupation numbers is observed. In Ref. [6] a finite temperature Gross-Pitaevskii equation is derived from the quantum many-body Hamiltonian for the Bose gas with this approximation in mind. An alternative route to similar equations of motion is possible via the use of the Wigner representation [7]. This approach may be more familiar to those from the quantum optics community.

Some of the first numerical calculations utilizing the GPE for finite temperature simulations were performed by Damle *et al*. [8] and Marshall *et al*. [9]. More recently there have been several calculations using the so-called "classical field" approximation. In particular we mention those of Gòral and co-workers [10–12], Sinatra and co-workers [13–16], and

the current authors [17,18]. These calculations are all related by the fact that they include no damping terms in the GPE, and thus rely on *ergodicity* for the system to thermalize. Classical field methods involving both damping and stochastic terms have been considered by Gardiner *et al*. [19], Stoof and Bijlsma [20], and Duine and Stoof [21].

While the qualitative results from previous work have been promising, there has been some difficulty in performing quantitative calculations using such methods, and in particular in determining the temperature of the system at equilibrium. We partially addressed this issue in previous work using a variety of methods to determine the temperature of our simulations [17,18]. The most reliable of these involved fitting time-averaged quasiparticle occupations and energies to the classical limit of the Bose-Einstein distribution function. However, this method relies on the existence of a basis that approximately diagonalizes the Hamiltonian (quasiparticles) for which energies and wave functions can be calculated in advance. This method is therefore only applicable in the realm of perturbation theory, and fails for even moderate temperatures in systems with large nonlinearities. Hence it is desirable to find a more widely applicable scheme for unambiguously determining the temperature of numerical simulations.

In a succinct yet insightful paper, Rugh [22] expressed the temperature of a classical Hamiltonian system in terms of a phase space expectation value of a suitable function of the canonical position and momentum coordinates [Eq. (19) of this paper.] Using the ergodic theorem, this expectation value over phase space can be interpreted as a dynamical average for a system in equilibrium, and immediately lends itself to applications in numerical calculations. Rugh developed this procedure further in [23], and generalized it to include systems with other conserved quantities in addition to the energy [24]. This generalization turns out to be crucial for the application of the method to the interacting Bose gas. Rugh's formula for the temperature has been applied to several sys-

*Electronic address: mdavis@physics.uq.edu.au

[†]Electronic address: sam@theory.phys.ucl.ac.uk

tems to date, for example, in the field of molecular dynamics. This has led to the notion of a configurational temperature for gases, which depends only on the spatial coordinates of the particles, in addition to the usual kinetic temperature which depends only on the momenta [25–27].

In this paper we apply the microcanonical formalism of Rugh to the BEC Hamiltonian to determine the temperature of numerical simulations of thermal Bose gases. The method is nonperturbative and does not rely on the existence of well-defined Bogoliubov quasiparticles. The paper is organized as follows. In Sec. II we briefly summarize the expression for the temperature and other derivatives of the microcanonical entropy, and describe their application to the BEC Hamiltonian. Section III presents our numerical results for our projected GPE (PGPE) system, while Sec. IV relates our calculations to other dynamical calculations of classical ϕ^4 field theory, as well as to calculations of the shift of the transition temperature for a homogeneous Bose gas. We conclude in Sec. V.

II. FORMALISM

A. Hamiltonian

We consider a classical system with M independent modes. The Hamiltonian can be written as $H = H(\mathbf{\Gamma})$, where $\mathbf{\Gamma} = \{\Gamma_i\} = \{Q_i, P_i\}$ is a vector of length $2M$ consisting of the canonical position and momentum coordinates. In these coordinates we define the gradient operator ∇ in terms of its components $\nabla_i = \partial/\partial \Gamma_i$.

In the notation of Rugh [24], the Hamiltonian H may have a number of independent first integrals, labeled by $F = F_1, \ldots, F_m$, that are invariant under the dynamics of H. We could define $F_0 = E$ and include the conserved energy with the other constants of motion in this notation, but for clarity we consider it separately. A particular macrostate of such a system can be specified by the values of the conserved quantities, labeled as $H = E, F_i = I_i$.

The expression for the temperature of such a system in the microcanonical ensemble is given by

$$\frac{1}{k_B T} = \left(\frac{\partial S}{\partial E} \right)_{F_i}, \tag{1}$$

where all other constants of motion are held fixed, and where the entropy is given by

$$e^{S/k_B} = \int d\mathbf{\Gamma} \, \delta[E - H(\mathbf{\Gamma})] \prod_i \delta[I_i - F_i(\mathbf{\Gamma})]. \tag{2}$$

In this case, the temperature of the system can be written as

$$\frac{1}{k_B T} = \langle \mathcal{D} \cdot \mathbf{X}(\mathbf{\Gamma}) \rangle, \tag{3}$$

where the angle brackets correspond to an ensemble average, and the components of the vector operator $\mathcal{D}$ are

$$\mathcal{D}_i = e_i \frac{\partial}{\partial \Gamma_i}, \tag{4}$$

where e_i can be chosen to be any scalar value, including zero. The vector field $\mathbf{X}$ can also be chosen freely within the constraints

$$\mathcal{D}H \cdot \mathbf{X} = 1, \quad \mathcal{D}F_i \cdot \mathbf{X} = 0, \quad 1 \leq i \leq m. \tag{5}$$

Geometrically this means that the vector field $\mathbf{X}$ has a nonzero component transverse to the $H = E$ energy surface, and is parallel to the surfaces $F_i = I_i$. The expectation value in Eq. (3) is over all possible states in the microcanonical ensemble; however, if the ergodic theorem is applicable then it can equally well be interpreted as a time average. For further details on the origin of this expression we refer the reader to Rugh's original papers [22–24], as well as to the derivations by Giardinà and Levi [28], Jepps *et al.* [26], and Rickayzen and Powles [29].

B. Dimensionless BEC Hamiltonian

The full quantum many-body Hamiltonian for the Bose gas in dimensionless form is

$$\tilde{H} = \int d^3\tilde{\mathbf{x}} \left[\nabla \tilde{\Psi}^\dagger(\tilde{\mathbf{x}}) \cdot \nabla \tilde{\Psi}(\tilde{\mathbf{x}}) + \tilde{V}(\tilde{\mathbf{x}}) \tilde{\Psi}^\dagger(\tilde{\mathbf{x}}) \tilde{\Psi}(\tilde{\mathbf{x}}) \right.$$
$$\left. + \frac{C_{nl}}{2} \tilde{\Psi}^\dagger(\tilde{\mathbf{x}}) \tilde{\Psi}^\dagger(\tilde{\mathbf{x}}) \tilde{\Psi}(\tilde{\mathbf{x}}) \tilde{\Psi}(\tilde{\mathbf{x}}) \right], \tag{6}$$

where $H = N\epsilon_L \tilde{H}$, N is the number of particles in the system, $\tilde{\mathbf{x}} = \mathbf{x}/L$, L is the unit of length, $\epsilon_L = \hbar^2/(2mL^2)$ is the unit of energy, m is the mass of the particles, and $\tilde{V}(\tilde{\mathbf{x}})$ is the dimensionless external potential if any is present. The dimensionless quantum Bose field operator $\tilde{\Psi}(\tilde{\mathbf{x}})$ is here normalized to 1, $\int d^3\tilde{\mathbf{x}} \langle \tilde{\Psi}^\dagger(\tilde{\mathbf{x}}) \tilde{\Psi}(\tilde{\mathbf{x}}) \rangle = 1$, and C_{nl} is the nonlinear constant defined as

$$C_{nl} = \frac{NU_0}{\epsilon_L L^3} = \frac{8\pi a N}{L}, \tag{7}$$

where a is the s-wave scattering length. In this expression we have assumed a high momentum cutoff and made use of the replacement of the true interatomic potential with the two-body T matrix $V(\mathbf{x}) \rightarrow U_0 \delta(\mathbf{x})$, where $U_0 = 4\pi\hbar^2 a/m$.

In Ref. [6] the field operator is split into a classical part and a quantum part, with the boundary determined by the requirement that the average occupation number $\langle N_k \rangle$ of modes below the cutoff satisfies $\langle N_k \rangle \gg 1$. Equations of motion were derived for the classical part, before taking the mean value. This resulted in the finite temperature Gross-Pitaevskii equation, which describes the evolution of a classical field coupled to an effective bath described by a quantum Boltzmann-like equation. This equation proves to be somewhat difficult to solve numerically, and in Refs. [17,18] we reported results focusing on a simplification we termed the projected Gross-Pitaevskii equation. This equation describes the evolution of a classical field only, with a cutoff at a given momentum or energy. It is identical to the usual GPE except that it evolves a wave function which is restricted to a finite-sized basis satisfying the classical condition $\langle N_k \rangle \gg 1$.

The PGPE for a homogeneous system is written explicitly for the homogeneous gas in Eq. (26) of this paper.

In this paper we wish to determine the temperature of the restricted system described by the evolution of the PGPE. Thus the Hamiltonian we consider is the classical version of Eq. (6) obtained by replacing the field operator $\widetilde{\Psi}(\widetilde{\mathbf{x}})$ with the classical field $\psi(\widetilde{\mathbf{x}})$, subject to the important restriction that $\psi(\widetilde{\mathbf{x}})$ is constructed from a finite number of low-energy modes. We can therefore write it in the form

$$\psi(\widetilde{\mathbf{x}}) = \sum_{k \in C} c_k \phi_k(\widetilde{\mathbf{x}}), \qquad (8)$$

where C labels the classical modes in the coherent region below the cutoff, as defined in [6].

C. Canonically conjugate position and momentum variables

We must now make a choice of the canonically conjugate coordinates of our Hamiltonian. As we are defining our classical field in a basis, it seems natural to convert to a basis representation. If we choose our basis to be that which diagonalizes the ideal gas Hamiltonian [the first two terms of Eq. (6)] we find

$$H = \sum_n \epsilon_n c_n^* c_n + \frac{C_{\mathrm{nl}}}{2} \sum_{mnpq} c_m^* c_n^* c_p c_q \langle mn|pq \rangle, \qquad (9)$$

where the matrix element is

$$\langle mn|pq \rangle = \int d^3\mathbf{x}\, \phi_m^*(\mathbf{x}) \phi_n^*(\mathbf{x}) \phi_p(\mathbf{x}) \phi_q(\mathbf{x}). \qquad (10)$$

The equation of motion for the $\{c_n\}$ is given by the PGPE. This problem can be mapped exactly to the one considered by Rugh by defining real, canonically conjugate coordinates Q_n and P_n,

$$Q_n = \frac{1}{\sqrt{2\epsilon_n}}(c_n^* + c_n), \quad P_n = i\sqrt{\frac{\epsilon_n}{2}}(c_n^* - c_n), \qquad (11)$$

with the corresponding inverse transformation

$$c_n = \sqrt{\frac{\epsilon_n}{2}}Q_n + \frac{i}{\sqrt{2\epsilon_n}}P_n, \quad c_n^* = \sqrt{\frac{\epsilon_n}{2}}Q_n - \frac{i}{\sqrt{2\epsilon_n}}P_n. \qquad (12)$$

With these definitions, the evolution of the c_n coefficients given by the PGPE maps exactly to the evolution of the coordinates Q_n and P_n given by Hamilton's equations. The PGPE is therefore in one-to-one correspondence with a classical microcanonical system, and its equilibrium properties can be studied using the wide variety of techniques that have been developed in classical statistical mechanics.

We have performed numerical calculations for the homogeneous PGPE, and so we use a plane wave basis where $\phi_n(\widetilde{\mathbf{x}}) = \exp(i\widetilde{\mathbf{k}}_n \cdot \widetilde{\mathbf{x}})$, $n = \{n_x, n_y, n_z\}$, and $\epsilon_n = |\widetilde{k}_n|^2 = (2\pi|n|)^2$. However, the method we describe is general and can be applied directly to inhomogeneous systems for BECs in magnetic and optical dipole traps.

Calculations on a grid

The implementation of a projection operator in the GPE is an essential feature of any classical simulation. While we have explicitly defined a projection operator in terms of a basis set, other authors have implicitly chosen a momentum cutoff by the use of a finite-size grid in their GPE simulations [11,12]. The method of temperature determination described in this paper can also be applied to these calculations, but with a different choice of position and momentum coordinates.

On a finite grid, the Hamiltonian (6) can be discretized in real space and the classical equivalent can be written as

$$H = h_x h_y h_z \sum_n \left[(\nabla \alpha_n)^2 + (\nabla \beta_n)^2 \right.$$
$$\left. + V_n(\alpha_n^2 + \beta_n^2) + \frac{C_{nl}}{2}(\alpha_n^2 + \beta_n^2)^2 \right], \qquad (13)$$

where $n \equiv \{n_x, n_y, n_z\}$ labels the grid point, h_x, h_y, h_z are the grid spacings for each axis, and we have defined $\psi_n = \alpha_n + i\beta_n$. In this case the appropriate position and momentum variables are

$$Q_n = \sqrt{2}\,\alpha_n, \qquad P_n = \sqrt{2}\,\beta_n. \qquad (14)$$

However, we believe that it is important to define the projector using a basis that is relatively well defined in energy *at the cutoff* (we stress that this does not mean that the basis has to be well defined in energy *below* the cutoff). It has previously been shown [30] that the single particle energy levels of a partially condensed system are essentially those of the trapping potential for energies $\epsilon \gtrsim E_R \approx 3\mu_C$, where μ_C is the condensate energy eigenvalue. Thus the above cutoff projector can be written

$$\hat{\mathcal{Q}}\{F(\mathbf{x})\} = \sum_{k \notin C} \phi_k(\mathbf{x}) \int d^3\mathbf{x}'\, \phi_k^*(\mathbf{x}') F(\mathbf{x}'), \qquad (15)$$

where the $\{\phi_k\}$ are the basis states appropriate to the potential, and the notation $k \notin C$ describes a summation over all modes above the energy cutoff E_R. As this basis is complete, the below cutoff projector is simply

$$\hat{\mathcal{P}} = \hat{I} - \hat{\mathcal{Q}}, \qquad (16)$$

which gives the result written explicitly in Eq. (27). We also require the classical condition

$$N_k = \frac{k_B T}{E_R - \mu} \gg 1 \qquad (17)$$

to hold at the cutoff and so for $E_R \approx 3\mu_C$ this should also be satisfied.

For a trapped Bose gas, the implicit momentum projector based on the finite-grid method is not at all well defined in energy at the cutoff, and we believe that this may lead to difficulties. However, this is yet to be invesigated numerically; for further discussion of this issue we refer the reader to [31].

D. Choice of vector field X

In order to satisfy the conditions (5) we can choose a vector field of the form

$$\mathbf{X} = a\mathcal{D}H + \sum_{i=1}^{m} b_i \mathcal{D}F_i, \qquad (18)$$

where the $m+1$ coefficients $\{a, b_i\}$ are determined by the $m+1$ simultaneous equations in Eq. (5). Due to the freedom in the choice of the vector operator $\mathcal{D}$ we can set any component of the length $2M$ vector $\mathbf{X}$ to zero. This turns out to be useful as the components corresponding to the momentum and position variables can be of different orders of magnitude. Two particular choices we make use of later are $\mathbf{X}_P$ with $\mathcal{D} = \mathcal{D}_P = \{0, \partial/\partial P_i\}$ and $\mathbf{X}_Q$ with $\mathcal{D} = \mathcal{D}_Q = \{\partial/\partial Q_i, 0\}$. These lead to two different calculations for the temperature that agree in general only if the system is in thermal equilibrium. This provides a useful check that the simulations have in fact thermalized.

In Rugh's first two papers [22,23] the only first integral considered was the energy, and he chose $\mathcal{D} \equiv \nabla$ which yielded the (dimensionless) formula

$$\frac{1}{T} = \left\langle \nabla \cdot \frac{\nabla H}{|\nabla H|^2} \right\rangle. \qquad (19)$$

For the BEC Hamiltonian we consider, however, there are other first integrals that must be taken into account. Most importantly, the evolution conserves the normalization of the wave function, but other first integrals that may occur are both the angular and linear momentum.

The effect of including these additional first integrals in the definition of the vector field $\mathbf{X}$ is to account for the energy that is associated with a conserved quantity and hence is unavailable for thermalization. This ensures that only the appropriate free energy is used to calculate the temperature. We conjecture that the same result can be achieved by first transforming to a coordinate system where the total angular and linear momenta, etc., are all zero and therefore do not contribute to the energy of the system. In fact, Rugh demonstrated this explicitly in [24] for a system of particles with a conserved center-of-mass motion.

An exception to this, however, is the conservation of normalization $N = \Sigma_n c_n^* c_n$. This must be considered explicitly because there is no coordinate system in which it can be made to vanish. The constraint on N means that the ground state of the system will, in general, have a finite energy. For example, a noninteracting gas in a harmonic trap of frequency ω must have at least the zero-point energy $\hbar\omega/2$ for each spatial degree of freedom. For a nonideal, homogeneous gas the restriction that at least one of the c_n must be nonzero means that there will always be a finite interaction energy associated with the ground state energy $\tilde{E}_0 = C_{\rm nl}/2$. These energy contributions are not accessible for thermalization, however, and including the normalization constraint allows them to be removed. We note, however, that the effect of this constraint is in general more complicated than a simple subtraction of the ground state energy (which could be achieved by hand) and depends on the definition of the operator $\mathcal{D}$ used to calculate the temperature, as shown below.

To deal with the normalization constraint, we need to choose a vector field $\mathbf{X}$ that satisfies Eqs. (5) with $F_1 = N = \Sigma_n c_n^* c_n$. The result is

$$\mathbf{X} = \frac{\mathcal{D}H - \lambda_N \mathcal{D}N}{|\mathcal{D}H|^2 - \lambda_N \mathcal{D}N \cdot \mathcal{D}H}, \qquad (20)$$

where the parameter

$$\lambda_N = \frac{\mathcal{D}N \cdot \mathcal{D}H}{|\mathcal{D}N|^2} \qquad (21)$$

looks similar to a chemical potential. For a system on a real space grid with $\mathcal{D} = \nabla$ and a Hamiltonian given by Eq. (13) we find that $\lambda_N = \mu_{\rm GPE}$, where $\mu_{\rm GPE}$ is the usual Gross-Pitaevskii form of the chemical potential, obtained from the Hamiltonian of Eq. (13) by doubling the interaction term. However, in general the expression of Eq. (21) does not have a simple interpretation.

Substituting Eq. (20) into Eq. (3) we find that our full expression for the temperature is

$$\frac{1}{T} = \left\langle \frac{\mathcal{D}^2 H - \lambda_N \mathcal{D}^2 N - \mathcal{D}\lambda_N \cdot \mathcal{D}N}{|\mathcal{D}H|^2 - \lambda_N(\mathcal{D}H \cdot \mathcal{D}N)} \right\rangle - \left\langle \frac{(\mathcal{D}H - \lambda_N \mathcal{D}N) \cdot [\mathcal{D}|\mathcal{D}H|^2 - (\mathcal{D}H \cdot \mathcal{D}N)\mathcal{D}\lambda_N - \lambda_N \mathcal{D}(\mathcal{D}H \cdot \mathcal{D}N)]}{[|\mathcal{D}H|^2 - \lambda_N(\mathcal{D}H \cdot \mathcal{D}N)]^2} \right\rangle. \qquad (22)$$

The second term in this expression is of order $1/M$, and so in many situations it can reasonably be neglected. However, we have calculated the full expression for all results presented in this paper.

E. Other thermodynamic quantities

The method described in this paper can also be used to calculate first derivatives of the microcanonical entropy with respect to any of the first integrals of the Hamiltonian [24]. In particular, we find that to calculate the quantity

$$\left(\frac{\partial S}{\partial F_j} \right)_{E, F_i}, \quad i \neq j,$$

the constraints on our vector field should be

$$\mathcal{D}H \cdot \mathbf{X} = 0, \quad \mathcal{D}F_i \cdot \mathbf{X} = 1, \quad \mathcal{D}F_j \cdot \mathbf{X} = 0, \quad i \neq j. \quad (23)$$

For the BEC Hamiltonian, we have

$$\frac{\mu}{k_B T} = -\left(\frac{\partial S}{\partial N}\right)_E, \quad (24)$$

and on implementing the required constraints we find that an appropriate vector field is that given by Eqs. (20) and (21) but with the roles of H and N reversed.

In addition, higher-order derivatives of the entropy can also be determined, making available quantities such as the specific heat c_{sp} of the system [23]. This quantity could in principle be calculated from the expression

$$\frac{1}{c_{\text{sp}}} = 1 - \frac{\langle \mathcal{D} \cdot (\mathbf{X} \mathcal{D} \cdot \mathbf{X}) \rangle}{\langle \mathcal{D} \cdot \mathbf{X} \rangle^2}, \quad (25)$$

where the vector $\mathbf{X}$ is determined by Eqs. (20) and (21). However, for the BEC Hamiltonian the expressions for such quantities are unreasonably complicated, and we do not consider them in this paper. Instead, higher derivatives will simply be obtained numerically once the temperature is determined.

III. NUMERICAL RESULTS

In this section we apply the formula Eq. (22) to data from simulations of the PGPE described in [17,18], as well as to many other simulations with a wider range of energies and nonlinear parameters C_{nl}. For a full description we refer the reader to Ref. [18]. Briefly, the calculations evolve the projected Gross-Pitaevskii equation [6] for the homogeneous gas in three dimensions

$$i\frac{\partial \psi(\widetilde{\mathbf{x}})}{\partial \tau} = -\widetilde{\nabla}^2 \psi(\widetilde{\mathbf{x}}) + C_{\text{nl}}\hat{\mathcal{P}}\{|\psi(\widetilde{\mathbf{x}})|^2 \psi(\widetilde{\mathbf{x}})\}. \quad (26)$$

The nonlinear constant is $C_{\text{nl}} = 2mNU_0/\hbar^2 L$, where N is the total number of particles in the volume, and L is the period of the system. Our dimensionless parameters are $\widetilde{\mathbf{x}} = \mathbf{x}/L$, wave vector $\widetilde{\mathbf{k}} = \mathbf{k}L$, energy $\widetilde{\epsilon} = \epsilon/\epsilon_L$, and time $\tau = \epsilon_L t/\hbar$, with $\epsilon_L = \hbar^2/(2mL^2)$. The projection operator $\hat{\mathcal{P}}$ excludes all components of the nonlinear term in the GPE outside the coherent region, and is defined by [cf. Eqs. (15) and (16)]

$$\hat{\mathcal{P}}\{F(\mathbf{x})\} = \sum_{k \in C} \phi_k(\mathbf{x}) \int d^3\mathbf{x}' \, \phi_k^*(\mathbf{x}')F(\mathbf{x}'), \quad (27)$$

where $\{\phi_k\}$ is an orthonormal basis appropriate to the problem. For the homogeneous system with periodic boundary conditions, the relevant basis is the plane wave states, and so this procedure is simply the application of a forward Fourier transform, removal of components with $\widetilde{k} > \widetilde{k}_c$, followed by the inverse transformation. The quantity $\widetilde{k}_c$ defines the momentum cutoff for the coherent region, and for all data presented in this paper we use $\widetilde{k}_c = 15 \times 2\pi$.

We begin with randomized initial fields $\psi(\widetilde{\mathbf{x}})$ with a given energy on a three-dimensional (3D) grid with 32 points in each dimension and evolve these until the field has reached equilibrium. We calculate all thermodynamic quantities from sampling 200 field configurations in equilibrium.

Cutoff dependence of simulations. The choice of momentum cutoff $\widetilde{k}_c = 15 \times 2\pi$ is motivated simply by computational convenience. It also allows for comparison of the Rugh method of temperature measurement with data from earlier calculations.

For a given initial energy, the resulting equilibrium temperature depends on the number of modes below the cutoff. This can be easily understood from the equipartition theorem —if more modes are present, less energy will be contained in each one and therefore the final temperature will be lower. Also, the dimensionless critical temperature for a system with a fixed normalization depends on the cutoff, as can be seen in the text beneath Eq. (28).

Work is currently in progress to develop a description of the modes above the cutoff and their coupling to the PGPE. The aim of this work is a complete computational method that will be insensitive to the exact position of the cutoff. Exploring and developing techniques for the nonperturbative classical field is an important part of this program, and we focus on this aspect of the problem in this paper.

Despite this, there are some equilibrium calculations which can be carried out immediately using an approximate treatment of the modes above the cutoff. We present results for one such calculation (the shift in T_c with interaction strength) in this paper. These results have only a weak dependence on the cutoff.

Use of the classical field method at T_c. The classical field can describe only modes that satisfy the high-occupation condition. But even at the critical temperature and above, the lowest-energy states will have the largest occupations—and for a wide range of parameters, many of these can satisfy $N_k \gg 1$. These are the modes that are responsible for critical behavior, such as the shift in T_c and the increase in specific heat. The remaining modes (that are not simulated) behave essentially as an ideal gas.

As a physical example, consider our simulations for $C_{\text{nl}} = 20\,000$. Choosing $L = 25\,\mu$m, and ^{87}Rb, this corresponds to approximately 3.8×10^5 atoms below the cutoff satisfying $N_k > 10$ at T_c of about 370 nK. There are about 1.3×10^6 atoms in total, with a total number density of 8.3×10^{13} cm^{-3}. Thus in this situation nearly 30% of the atoms are simulated by the PGPE.

A. Comparison of methods of temperature determination

As described in Sec. II D there are many choices of the operator $\mathcal{D}$ that may be used in Eq. (22). The resulting calculations give the same temperature only if the system is in equilibrium, so this provides an important confirmation that the system has thermalized. In this paper we consider two cases $\mathcal{D}_Q = \{\partial/\partial Q_i, 0\}$ and $\mathcal{D}_P = \{0, \partial/\partial P_i\}$, and we refer to the temperatures calculated from these operators as T_Q and T_P, respectively. Allowing Q or P derivatives only in the
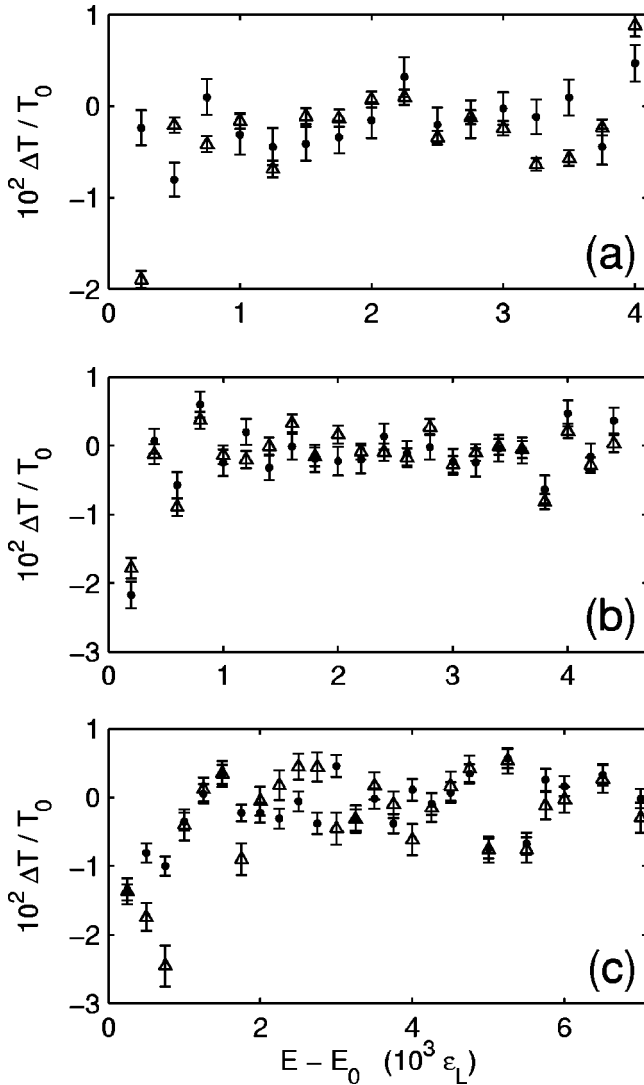
FIG. 1. Plot of the relative differences of simulation temperatures T_Q and T_P calculated from Eq. (22) with temperatures T_0 determined from the same data plotted in Fig. 9 of Ref. [18]. Open triangles, $\Delta T = T_P - T_0$; black dots, $\Delta T = T_Q - T_0$. (a) $C_{nl} = 500$, (b) $C_{nl} = 2000$, (c) $C_{nl} = 10\,000$.
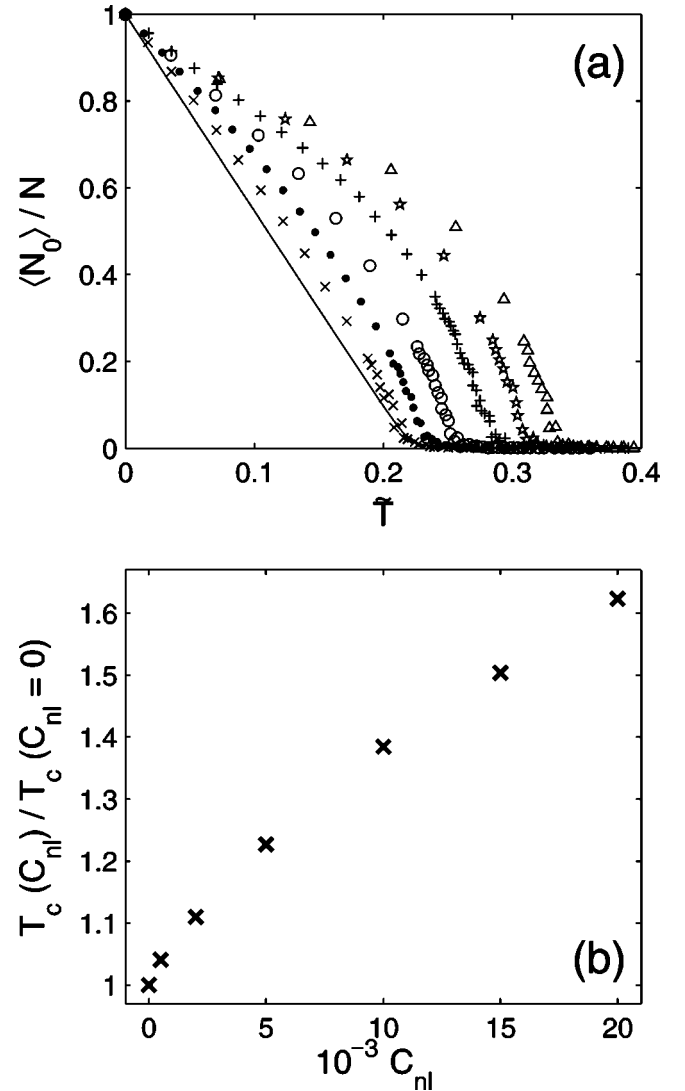

FIG. 2. (a) Plot of the condensate fraction versus temperature for a number of interaction strengths. Solid line, $C_{nl} = 0$; crosses, $C_{nl} = 500$; solid dots, $C_{nl} = 2000$; open circles, $C_{nl} = 5000$; pluses, $C_{nl} = 10\,000$; stars, $C_{nl} = 15\,000$; open triangles $C_{nl} = 20\,000$. (b) Plot of the transition temperature versus interaction strength. The transition temperature is determined by the method of Binder cumulants as described in the text.

separate definitions of the operator $\mathcal{D}$ simplifies the calculation of Eq. (22) due to the elimination of mixed derivatives.

We begin by comparing T_Q and T_P with previous results from Ref. [18]. In this earlier work we obtained temperatures using three different methods, two based on Bogoliubov quasiparticles and perturbation theory, and a third nonperturbative calculation. This third method did not have a firm theoretical basis; however, we showed that the results were consistent with the two other calculations in their regime of validity, and gave reasonable results more generally. Figure 1 shows the relative differences between the simulation temperatures T_Q and T_P calculated from Eq. (22) and the temperatures T_0 determined from the earlier method 3. The simulation data used are the same as those plotted in Fig. 9 of Ref. [18].

We can see from Fig. 1 that only a small number of points differ by more than 1% from the previously determined values, and even these would be hard to detect on a plot of the

absolute temperatures. These results therefore validate our earlier nonperturbative method for temperature determination in a homogeneous system (described in Sec. VI D of Ref. [18]). Figure 1 also shows that in general the values of T_Q and T_P agree with each other within their error bars. The error is determined from the standard deviation of the expectation value of Eq. (22) divided by the square root of the number of samples (in this case 200). This estimate assumes Gaussian statistics, which seems reasonable when the distribution of values is plotted as a histogram; however, it may underestimate the actual error somewhat. The agreement between these distinct determinations of temperature confirms their validity and provides important further evidence that the PGPE evolves randomized initial states to a thermodynamic equilibrium consistent with the microcanonical ensemble.

B. Shift of the transition temperature

Figure 2(a) plots the equilibrium temperatures and condensate fractions for several series of simulations with different nonlinearities C_{nl}, as well as for the ideal gas. These can be interpreted to be simulations at a fixed density with a varying scattering length. It is immediately obvious that qualitatively the transition temperature increases with increasing nonlinearity, and this was noted in [18]. Many more simulations have been performed for this paper, and we now have a much more reliable measure of temperature. Thus we can now look at the shift of the critical temperature with the nonlinear parameter C_{nl} for our PGPE system.

We can calculate the transition temperature for a noninteracting gas with equipartion occupation numbers and a momentum cutoff k_c in the continuum limit via

$$N = N_0 + \int_0^{k_c} \frac{d^3\mathbf{k}}{(2\pi)^3} \frac{k_B T}{\hbar^2 k^2/(2m) - \mu}. \qquad (28)$$

We find that the dimensionless critical temperature for a homogeneous PGPE system with a momentum cutoff of $k_c = 2\pi\kappa/L$ is $\tilde{T}_c(C_{nl}=0) = \pi/\kappa$, where the dimensionless temperature is defined by $\tilde{T} = k_B T/(N\epsilon_L)$.

Identifying the critical point in a finite-sized system with interactions, however, is somewhat more difficult. Here we make use of the method of Binder cumulants [32], which have been used in other finite-size calculations for the Bose gas [33]. We note that the theory behind Binder cumulants is derived entirely from canonical statistical mechanics. However, the calculations of Caiani et al. [34,35] suggest that it is valid as a numerical tool in the microcanonical ensemble, and we shall follow their lead. The Binder cumulant can be written as

$$C = \frac{\langle N_0^2 \rangle}{\langle N_0 \rangle^2}, \qquad (29)$$

where N_0 is the population of the zero-momentum condensate mode in our simulations. This quantity changes smoothly from 1 for the condensed system (ordered phase) to 2 for the uncondensed system (disordered phase), with the width of the transition region decreasing with increasing lattice size. However, in lattice field theory the chemical potential at which curves of C vs T intersect for different lattice sizes is universal for a given universality class, which is three-dimensional XY for our system. It has been calculated by Campostrini et al. [36] that this critical value is $C_c = 1.2430(1)(5)$, where the first number in parentheses is due to statistical errors and the second is due to systematic errors.

We therefore determine the critical temperature from our simulations by finding the energy at which the Binder cumulant takes the value C_c in equilibrium. Due to our limited statistics from 200 field samples, the results are somewhat noisy, but we are able to identify $\tilde{T}_c$ for the simulations to an accuracy of approximately 1%.

We note that for the case of $C_{nl}=20\,000$ the predicted shift in critical temperature is more than 60%. However, this
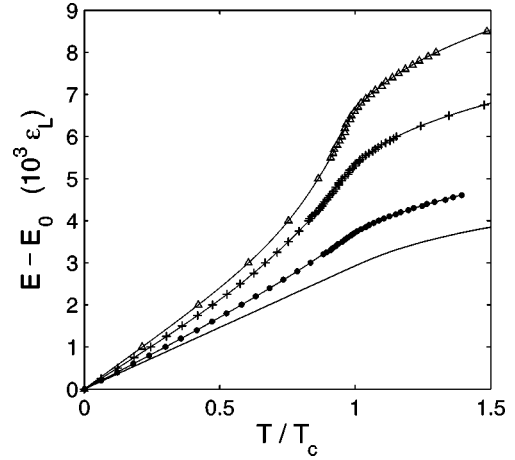

FIG. 3. The system energy plotted against the temperature, scaled in units of the critical temperature T_c so that the curves are distinct in the linear region. Solid line, $C_{nl}=0$; solid dots, $C_{nl}=2000$; pluses, $C_{nl}=10\,000$; open triangles, $C_{nl}=20\,000$. The lines passing through the numerical data points are the smoothing spline fits.

corresponds to the shift in *dimensionless* temperature of the low-energy states, not the shift in the critical temperature of the complete system, which will be smaller. This will be discussed in more detail in Sec. IV B.

C. Calculation of the specific heat

Although the specific heat can theoretically be determined by a similar procedure to that used for the temperature, the actual formulas are rather complicated and difficult to calculate. Instead, in this section we use numerical methods to calculate curves for the specific heat.

The calculation of numerical derivatives is difficult for data with statistical errors. Here we have applied a smoothing spline fitting technique to the raw numerical data for energy and temperature and calculated the derivative from this fit. Examples of the spline fits to the numerical data are plotted in Fig. 3.

The specific heat curves calculated from the data in Fig. 3 are shown in Fig. 4(a). The units of the vertical axis are scaled by the specific heat of the ideal Bose gas for the same system at $T=0$. We can see that there is a strong peak near the critical temperature that increases with increasing C_{nl}. Scaling theory for critical points in the thermodynamic limit suggests that the specific heat will be peaked at the phase transition. In our case the peak is not exactly at T_c, as perhaps would be expected. We presume that this is due to to a combination of finite-size effects and numerical errors in the fitting procedure, which we estimate to be a few percent. Similar behavior has also been noted in [34]. Figure 4(b) shows the maximum value of the specific heat plotted versus C_{nl}.

IV. RELATION TO OTHER WORK

A. Dynamics of ϕ^4 lattice field theory

The results presented in this paper for the homogeneous Bose gas have many similarities to classical ϕ^4 lattice field
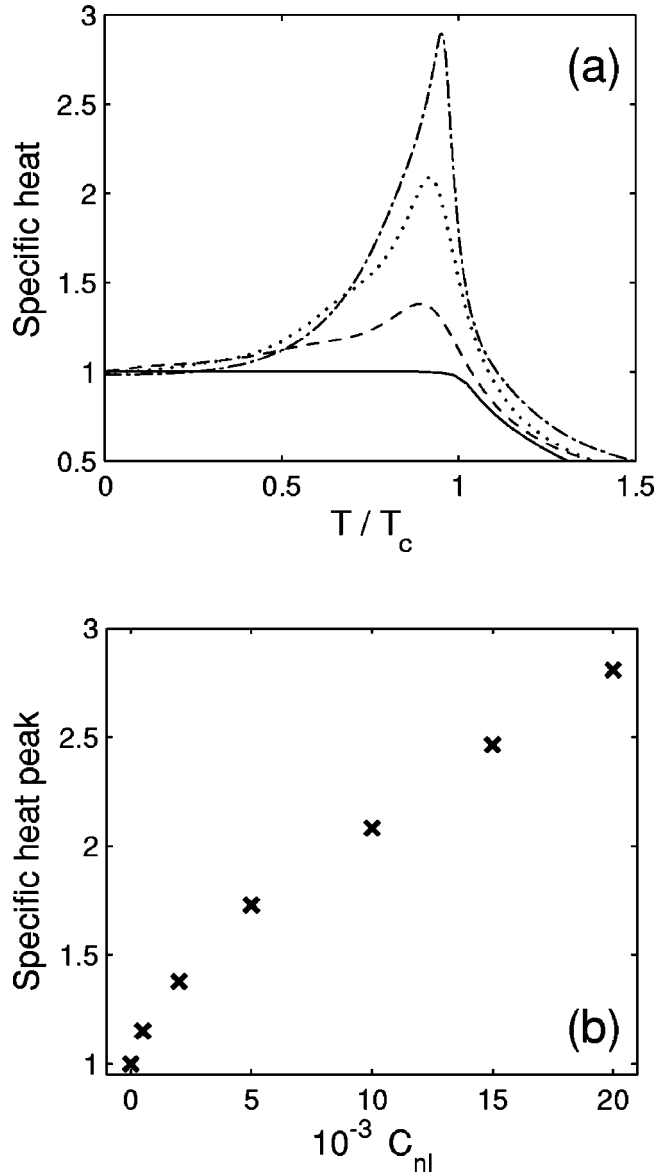
FIG. 4. (a) The numerically calculated specific heat curves for various interaction strengths. The peaks occur at temperatures a few percent below the identified transition temperature. We estimate the error for these curves to be of the order of a few percent. Solid black line, $C_{nl}=0$; dashed line, $C_{nl}=2000$; dotted line, $C_{nl}=10\,000$; dash-dot line, $C_{nl}=20\,000$. (b) The maximum value of the specific heat plotted versus the dimensionless interaction strength C_{nl}. For both (a) and (b), the specific heat is plotted relative to the corresponding value at $T=0$, and so the quantities are dimensionless.

theory, which is often studied in relation to second-order phase transitions. In such studies the field is discretized on a lattice with the spatial derivatives of the Hamiltonian being approximated by finite difference methods. Monte Carlo simulations are then performed to study the thermodynamics.

However, there have also been "molecular dynamic" simulations of such field theories, and in particular we note the work of Caiani *et al.*, who considered the phase transition via dynamical simulation of the ϕ^4 model in both two [35] and three dimensions [34]. Their equations of motion are

distinct from those of this paper by virtue of being second order in time. Their paradigm Hamiltonian in d dimensions is

$$H[\phi]=\int d^d\mathbf{x}\frac{1}{2}\pi^2(\mathbf{x})+\frac{J}{2}[\nabla\phi(\mathbf{x})]^2+\frac{1}{2}\phi^2(\mathbf{x})+\frac{\lambda}{4}\phi^4(\mathbf{x}),$$
(30)

with the canonical position variables $\phi(\mathbf{x})$ and conjugate momenta $\pi(\mathbf{x})=\dot{\phi}(\mathbf{x})$, where ϕ is a vector quantity with up to four dimensions. We note that as this Hamiltonian is of the form $H=\pi^2/2+V(\phi)$, both the temperature and specific heat of these simulations can be calculated from expectation values of the kinetic energy. This is not possible for the Hamiltonian we consider in this paper where the interaction term mixes powers of the position and momentum coordinates.

Also, in Ref. [35] the parameters used were $J=1,\lambda=0.6$, and for Ref. [34] the values $J=1$, $\lambda=0.1$, and $\lambda=4$ are specifically mentioned. Thus these calculations appear to be in quite a different regime from the results presented here. Despite these differences, however, it seems that many of their numerical results are qualitatively similar to ours.

B. Shift of T_c in the continuum limit

The results presented in this work can also be connected to the issue of the shift in the transition temperature for the homogeneous Bose gas, which has been the subject of a number of recent papers. In the weak interaction limit the shift ΔT_c has the form

$$\frac{\Delta T_c}{T_{c0}}=can^{1/3},$$
(31)

where T_{c0} is the transition temperature for the ideal gas, n is the density, a is the s-wave scattering length, and c is a dimensionless constant. The value of c cannot be determined by perturbation theory as this breaks down at second-order phase transitions due to infrared divergences. There have been several calculations of the value of c, differing by up to an order of magnitude and even in sign (see the summary in [37]).

The dimensionless constant c has recently been determined via Monte Carlo calculations by Arnold and Moore [33,37] and by Kashurnikov *et al.* [38] to be $c=1.32\pm0.02$ and $c=1.29\pm0.05$, respectively. These calculations were carried out via classical ϕ^4 field theory, which can be systematically matched to the problem of the homogenous interacting Bose gas. The Monte Carlo calculations proceeded by sampling the classical action

$$\frac{S}{\beta}=\int d^3\mathbf{x}\left[\psi^*(\mathbf{x})\left(-\frac{\hbar^2\nabla^2}{2m}-\mu_{\text{eff}}\right)\psi(\mathbf{x})+\frac{U_0}{2}|\psi(r)|^4\right],$$
(32)

on a lattice at a fixed temperature T, where $\beta=(k_BT)^{-1}$. The value of μ_{eff} was adjusted until the critical point was reached, and thus the shift in critical density $n_c=\langle|\psi|^2\rangle$ from the ideal gas value n_{c0} could be measured. The shift in critical temperature at a fixed density can then be determined from

$$\frac{\Delta T_c}{T_{c0}} = -\frac{2}{3}\frac{\Delta n_c}{n_{c0}}, \qquad (33)$$

which is easily derived from the formula for the critical temperature of the ideal gas. While this procedure seems straightforward, in practice it is necessary to give careful consideration to finite-size effects in the calculation—see Ref. [33] for a detailed discussion of these matters.

The results of simulations similar to those presented here can also be used to calculate a value for c, as we are also sampling the thermodynamic functions of classical ϕ^4 field theory. The Monte Carlo calculations fix the temperature and adjust the value of μ_{eff} in Eq. (32) which then determines the normalization of the field. In our calculations, we adjust the energy of the initial state to find the critical point and determine the temperature using the method described above. Our simulations have a fixed normalization, but the dimensionless temperature $\tilde{T} \propto T/N$, so for a given value of C_{nl} we can interpret our results as being at a fixed temperature and a varying density.

The main difference between the methods is the manner in which field configurations are sampled. The Monte Carlo methods can use the most efficient update possible, as long as the samples are canonical at a given temperature. Our calculations solve for the evolution of a microcanonical field and use the theorem of ergodicity to generate an ensemble. We have one minor advantage in that our momentum cutoff is spherically symmetric, whereas the Monte Carlo calculations simulate the first Brillouin zone of the lattice. However, the molecular dynamics method suffers from critical slowing down—as the energy of the highest modes is proportional to k^2, we require time steps of order $\delta t = 1/k_c^2$, where k_c is the momentum cutoff. Thus our simulations are disproportionately less efficient for larger grids compared to the Monte Carlo calculations and will not be able to generate results as accurately for a given computation time [39]. Nonetheless, we can use our simulations to confirm qualitatively the results of the Monte Carlo analysis, providing an independent demonstration of the validity and potential usefulness of our temperature determination method.

As a simplified illustration, we follow through the logical procedure that would be required to calculate a value for c. To consider the shift in the critical point, we can consider the shift in the critical density given a fixed critical temperature T_0. In our numerical simulations we keep $C_{\mathrm{nl}} = 8\pi a N_{\mathrm{below}}/L$ fixed and measure a shifted critical temperature

$$\tilde{T}_c = \frac{k_B T_0}{N_{\mathrm{below}}\epsilon_L}. \qquad (34)$$

Here N_{below} is the number of particles below the cutoff. If we fix the critical temperature at T_0 as well as the system size L (and hence ϵ_L), we can interpret the increase in the dimensionless quantity $\tilde{T}_c$ as a decrease in the value of N_{below} and hence a decrease in the critical density. The most important point to note is that as long as we have $k_c \gg k_0$, where k_0 labels the division between quasiparticle- and particlelike ex-
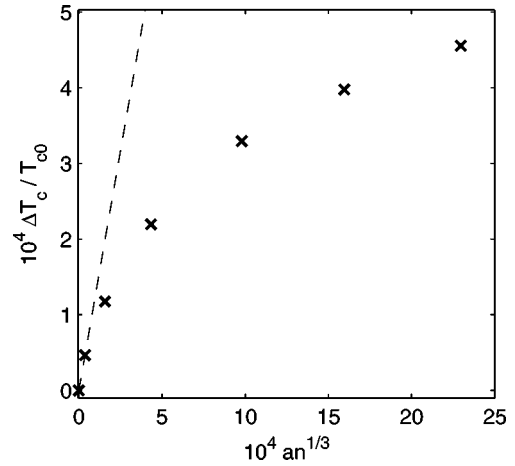

FIG. 5. Shift in the critical temperature with interaction strength determined from the results presented in this paper with $N_{\mathrm{below}}(C_{\mathrm{nl}}=0)=10^{10}$. The dashed line is a linear fit to the first two data points and this has a slope of 1.3 ± 0.4.

citations at the transition temperature, then particles above the cutoff will not be significantly affected by the change in the interaction strength.

We therefore calculate $N_{\mathrm{above}} = N_{\mathrm{tot}} - N_{\mathrm{below}}$ for the ideal gas, where N_{tot} is the total number of particles. This will be a constant as long as $k_c \gg k_0$. We can then calculate $N_{\mathrm{below}}(C_{\mathrm{nl}})$ and hence the shift in the critical density from the simulation data, and by using the relation of Eq. (33), we obtain the shift in the critical temperature.

This can then be plotted against $an^{1/3}$ and the slope at the origin determines the coefficient c. This plot is given in Fig. 5, where we have set $N_{\mathrm{below}}(C_{\mathrm{nl}}=0)=10^{10}$. We note that the method does not depend on the value chosen for $N_{\mathrm{below}}(C_{\mathrm{nl}}=0)$ as long as it is large enough that $\langle N_k \rangle \gg 1$ is well satisfied.

By fitting a straight line to the first two points as illustrated in Fig. 5, we get an estimate for the coefficient

$$c = 1.3\pm0.4, \qquad (35)$$

where the error specified is due to the uncertainty in the value of T_c for the data point. This agrees with the value determined in Refs. [37,38] — a result that should be treated with caution. The correct value of c will be reached only in the limit of large volume and small lattice spacing, and we believe we have not reached this regime. For comparison with the results of Arnold and Moore, for our first data point we have $Lu \approx 325$ and $ua_{\mathrm{latt}} \approx 10.2$, where $u = 3\tilde{T}C_{\mathrm{nl}}/L$ and $a_{\mathrm{latt}} = L/32$. Our other data points have values for these quantities that are much larger than this. Arnold and Moore suggest that $Lu \gtrsim 400$ and $ua_{\mathrm{latt}} \lesssim 6$ are necessary to get an accurate result for c without a finite-size scaling analysis [33,39].

We could potentially improve our results by performing such a finite-sized scaling analysis, but there is little reason to do so given the greater accuracy obtained in Refs. [37,38]. The purpose of this calculation is to demonstrate a useful application of our temperature determination with the PGPE in a nonperturbative regime. In this regard the qualitative

agreement with earlier more involved and specialized calculations provides a pleasing confirmation of the general validity of the method.

V. CONCLUSIONS

We have shown that the projected Gross-Pitaevskii equation can be exactly mapped to Hamilton's equations of motion for canonically conjugate position and momentum variables. Using this mapping we have described how to utilize the microcanonical thermodynamic method of Rugh [24] to measure the temperature of PGPE simulations in the nonperturbative regime. This method agrees with previous calculations described in Ref. [18], but has a rigorous theoretical justification and wider applicability. Using this approach, we have quantitatively measured the shift in the critical temperature for condensation with the nonlinear constant C_{nl}. We have also observed that the specific heat reaches a maximum near the transition point as expected from the theory of continuous phase transitions and that the peak value increases with the nonlinearity. Finally, we have made a connection between these calculations and Monte Carlo simulations that have determined the shift in the critical temperature with scattering length of the homogeneous Bose gas in the continuum limit. This is further evidence that the projected GPE should be valid for dynamical calculations through the critical region as long as the condition on the occupation numbers is satisfied.

[1] F. Dalfovo, S. Giorgini, L. P. Pitaevskii, and S. Stringari, Rev. Mod. Phys. **71**, 463 (1999), and references within.

[2] B. V. Svistunov, J. Mosc. Phys. Soc. **1**, 373 (1991).

[3] Yu. Kagan, B. V. Svistunov, and G. V. Shlyapnikov, Zh. Éksp. Teor. Fiz. **101**, 528 (1992) Sov. Phys. JETP **75**, 387 (1992).

[4] Yu. Kagan and B. V. Svistunov, Zh. Éksp. Teor. Fiz. **105**, 353 (1994) [JETP **78**, 187 (1994)].

[5] Yu. Kagan and B. V. Svistunov, Phys. Rev. Lett. **79**, 3331 (1997).

[6] M. J. Davis, R. J. Ballagh, and K. Burnett, J. Phys. B **34**, 4487 (2001).

[7] M. J. Steel, M. K. Olsen, L. I. Plimak, P. D. Drummond, S. M. Tan, M. J. Collett, D. F. Walls, and R. Graham, Phys. Rev. A **58**, 4824 (1998).

[8] K. Damle, S. N. Majumdar, and S. Sachdev, Phys. Rev. A **54**, 5037 (1996).

[9] R. J. Marshall, G. H. C. New, K. Burnett, and S. Choi, Phys. Rev. A **59**, 2085 (1999).

[10] K. Gòral, M. Gajda, and K. Rzążewski, Opt. Express **8**, 92 (2001).

[11] K. Gòral, M. Gajda, and K. Rzążewski, Phys. Rev. A **66**, 051602 (2002).

[12] H. Schmidt, K. Gòral, F. Floegel, M. Gajda, and K. Rzążewski, J. Opt. B: Quantum Semiclassical Opt. **5**, 96 (2003).

[13] A. Sinatra, Y. Castin, and C. Lobo, J. Mod. Opt. **47**, 2629 (2000).

[14] A. Sinatra, C. Lobo, and Y. Castin, Phys. Rev. Lett. **87**, 210404 (2001).

[15] A. Sinatra, C. Lobo, and Y. Castin, J. Phys. B **35**, 3599 (2002).

[16] C. Lobo, A. Sinatra, and Y. Castin, e-print cond-mat/0301628.

[17] M. J. Davis, S. A. Morgan, and K. Burnett, Phys. Rev. Lett. **87**, 160402 (2001).

[18] M. J. Davis, S. A. Morgan, and K. Burnett, Phys. Rev. A **66**, 053618 (2002).

[19] C. W. Gardiner, J. R. Anglin, and T. I. A. Fudge, J. Phys. B **35**, 1555 (2002).

[20] H. T. C. Stoof and M. J. Bijlsma, J. Low Temp. Phys. **124**, 431 (2001).

[21] R. A. Duine and H. T. C. Stoof, Phys. Rev. A **65**, 013603 (2001).

[22] H. H. Rugh, Phys. Rev. Lett. **78**, 772 (1997).

[23] H. H. Rugh, J. Phys. A **31**, 7761 (1998).

[24] H. H. Rugh, Phys. Rev. E **64**, 055101 (2001).

[25] B. D. Butler, G. Ayton, O. G. Jepps, and D. J. Evans, J. Chem. Phys. **109**, 6519 (1998).

[26] O. G. Jepps, G. Ayton, and D. J. Evans, Phys. Rev. E **62**, 4757 (2000).

[27] J. Delhommelle and D. J. Evans, J. Chem. Phys. **114**, 6229 (2001); **114**, 6236 (2001).

[28] C. Giardinà and R. Levi, J. Stat. Phys. **91**, 1027 (1998).

[29] G. Rickayzen and J. G. Powles, J. Chem. Phys. **114**, 4333 (2001).

[30] C. W. Gardiner and P. Zoller, Phys. Rev. A **58**, 536 (1998).

[31] C. W. Gardiner and M. J. Davis, e-print cond-mat/0308044 (2003).

[32] K. Binder, Z. Phys. B: Condens. Matter **43**, 119 (1981).

[33] P. Arnold and G. D. Moore, Phys. Rev. E **64**, 066113 (2001).

[34] L. Caiani, L. Casetti, and M. Pettini, J. Phys. A **31**, 3357 (1998).

[35] L. Caiani, L. Casetti, C. Clementi, G. Pettini, M. Pettini, and R. Gatto, Phys. Rev. E **57**, 3886 (1998).

[36] M. Campostrini, M. Hasenbusch, A. Pelissetto, P. Rossi, and E. Vicari, Phys. Rev. B **63**, 214503 (2001).

[37] P. Arnold and G. Moore, Phys. Rev. Lett. **87**, 120401 (2001).

[38] V. A. Kashurnikov, N. V. Prokof'ev, and B. V. Svistunov, Phys. Rev. Lett. **87**, 120402 (2001).

[39] G. Moore and P. Arnold (private communication).